Swirling spray flames dynamical blow out induced by transverse acoustic oscillations

Clément Patat, Françoise Baillot, Jean-Bernard Blaisot, Éric Domingues, Guillaume Vignat, Preethi Rajendram Soundararajan, Antoine Renaud, D. Durox, Sébastien Candel

Version of Record: https://www.sciencedirect.com/science/article/pii/S1540748922003170
Manuscript_289fd995ba9c1ffdf8b128760211bd25

Swirling spray flames dynamical blow out induced by transverse acoustic oscillations

Clément Patat[a], Françoise Baillot[a,*], Jean-Bernard Blaisot[a], Éric Domingues[a], Guillaume Vignat[b], Preethi Rajendram Soundararajan[b], Antoine Renaud[b], Daniel Durox[b], Sébastien Candel[b,*]

[a] *CORIA UMR 6614 CNRS, Site Universitaire du Madrillet, 76801 Saint Etienne du Rouvray, France*
[b] *EM2C lab, CNRS and CentraleSupélec, University Paris-Saclay, 91192 Gif-sur-Yvette, France*

Abstract

Recent experiments on a laboratory scale annular system comprising multiple injectors (namely, MICCA-Spray), indicate that combustion instabilities coupled with azimuthal modes may induce large amplitude oscillations, which under certain conditions, lead to blow out of some of the flames established in the system, a phenomenon designated as dynamical blow out (DBO). An attempt is made in the present investigation to reproduce this phenomenon in a linear array of injectors (namely, TACC-Spray), where the acoustic field is externally applied to flames established by injector units that are identical to those used in the annular combustor. The acoustic field is generated by driver units placed on the lateral sides of a rectangular cavity. The pressure level induced in TACC-Spray can reach a peak value of 1700 Pa in a frequency range extending from 680 to 780 Hz, which corresponds to the typical frequency of azimuthal instabilities observed in the annular system. A theoretical model based on dimensional analysis serves to guide the choice of operating conditions that may lead to the DBO phenomenon. Experiments carried out in TACC-Spray and MICCA-Spray are then used to determine the DBO boundary, define the conditions that need to be fulfilled to observe this phenomenon, and gather high-speed visualizations providing some insights on the mechanisms that induce blow out.

Keywords: Flame blow out; Transverse acoustics; Swirling spray flames

1. Introduction

When combustion instabilities arise in a real system, they induce high levels of pressure oscillations, mechanical vibrations, cyclic fatigue, enhanced heat fluxes to the combustor walls, and in extreme cases, structural degradation possibly leading to failure. In some instances, the oscillation can be so strong that it gives rise to flame flashback. Understanding, predicting and controlling these dynamical processes have been constant objectives of a considerable amount of fundamental and more applied research (see for example the reviews [1–4]). One aspect that is less well documented is the possible extinction of flames submitted to high amplitude oscillations accompanying certain types of instabilities. This intriguing phenomenon is the subject of the present investigation. It was recently observed when the coupling between acoustics and combustion involves an azimuthal mode. It is then logical to briefly review the literature specifically dealing with such instabilities. Most of these investigations have been carried out during the more recent period in annular systems. These are typically found in aircraft engines and gas turbines. Since the perimeter is usually the largest dimension in these annular geometries, azimuthal modes feature the lowest eigenfrequencies, which fall in the range where combustion is most sensitive to disturbances. As a consequence, these systems are susceptible to instabilities coupled by azimuthal modes. Experimental studies [5–13] have been accompanied by theoretical investigations [14–22] and by some remarkable large eddy simulations [23, 24].

On the experimental level, much of the data originates from two laboratory scale annular systems with optical access to the combustion region, one of these facilities was initially located in Cambridge and later in NTNU [7, 8], while the other (MICCA-Spray) has been operated at EM2C lab [10, 12, 13, 25, 26]. These two systems reproduce, in an idealized fashion, conditions prevailing in gas turbines and jet engines. They feature multiple injectors arranged in a circular array in the chamber backplane. While the first is essentially fed with premixed reactants (air and ethylene), MICCA-Spray may be operated with premixed air and propane or may be fed with liquid fuel (n-heptane or dodecane) that is injected in the form of sprays. Flame stabilization in the Cambridge-NTNU system is assured by central bluff bodies with a relatively low swirl number. In the MICCA-Spray device, investigations have been carried out with swirling injectors fed by premixed reactants and more recently by liquid fuels atomized as a spray of droplets.

These experimental facilities have provided considerable insight on the processes driving and coupling azimuthal instabilities. Recent combustion instability experiments carried out in MICCA-Spray have shown that flames could be extinguished when the oscillation amplitude was taking large values, typically in excess of 2% to 3% of the chamber pressure

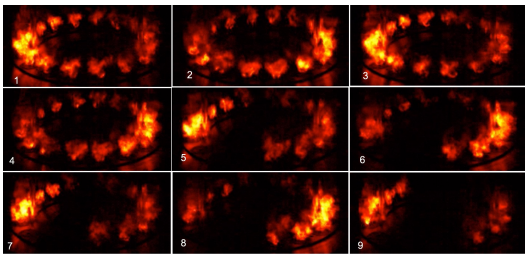

Fig. 1: Dynamical blow out in the annular combustor MICCA-Spray. Images show the successive extinctions of the flames located near the pressure nodal line of a standing 1A1L azimuthal mode of the system as the acoustic pressure amplitude grows up and reaches 4000 Pa (see [27] for further experimental data).

[13]. Under these conditions, some of the flames established in the combustor were blown out, as illustrated in Fig. 1 for an acoustic pressure amplitude of 4000 Pa. Further analysis indicated that this partial blow out occurred in the vicinity of the pressure nodal line, where the transverse velocities associated with the azimuthal mode reach their maximum level, inducing an intense sweeping motion. Under these conditions, the combustion process is disrupted, inducing a complete extinction of flames established near the nodal line. The time duration of this phenomenon was found to encompass about 100 ms, corresponding to about 70 cycles of oscillation. After this blow out, the amplitude of oscillation in the chamber diminishes and the flames are established again. The process may then be repeated, leading to a new partial blow out. This phenomenon, designated in what follows as dynamical blow out (DBO) was the subject of a further investigation [27], and it was found that the flame extinction was accompanied by a notable distortion of the pressure field and simultaneously by a shift in the resonance frequency. It was also possible to estimate the velocity fluctuation amplitude corresponding to the initial flame extinction.

The objective of the present study is to pursue the analysis of the DBO by making use of a configuration designated as TACC-Spray, in which the acoustic modulations are imposed to the flame by external means. In essence, this consists in placing a linear array of swirl spray injectors in a rectangular chamber, which consists in an unwrapped sector of the annular combustor MICCA-Spray (as explained in Fig. 2). A transverse acoustic mode is generated by driver units located on the lateral boundaries of this facility. The central flame formed in this injector array can then be placed at the pressure nodal line, corresponding to the maximum transverse acoustic velocity. It is then possible to augment the level of oscillation and examine the process leading to flame blow out. One advantage of this procedure is that the acoustic level is fully controlled, thus facilitating the detailed investigation of the DBO. It is in particular possible to decouple the level of the acoustic mode and the combustion opera-

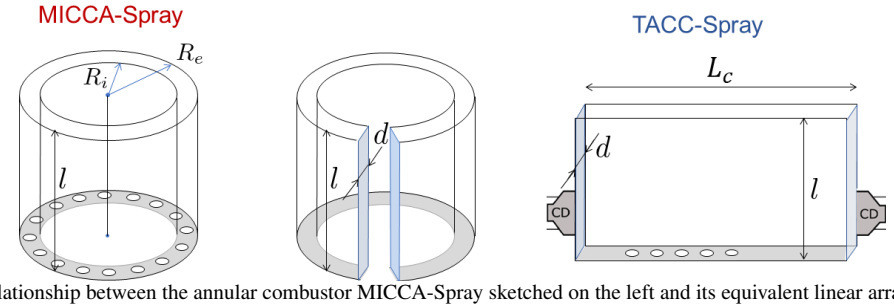

Fig. 2: Relationship between the annular combustor MICCA-Spray sketched on the left and its equivalent linear array equipped with lateral driver units, TACC-Spray, which consists in an unwrapped sector of the annular combustor. CD: driver units.

tional conditions, a feature that is not available in the annular combustor MICCA-Spray where the acoustic level is governed by the coupling between acoustics and combustion.

The idea of using linear arrays of injectors to represent a sector of an annular system is not new. Such arrays have already been employed by O'Connor and Lieuwen [28, 29], by Kwong and Steinberg [30] or by Lespinasse et al. [31, 32]. In these last references, a premixed "V" flame is submitted to a transverse acoustic field. When placed at the pressure antinodal line, where the pressure reaches maximum levels of fluctuations, the flame executes an axial motion. There are also nonlinear features with lateral ejections of fluid at the injector outlet [32]. In the vicinity of the pressure nodal line, the flame is periodically swept back and forth in the transverse direction. If the injection unit comprises a swirler, helical perturbations result from the interaction of the transverse acoustic velocities with the shear regions and with the vortex breakdown process [28, 29]. Transverse waves acting on the upstream side of the injector unit may also induce a rotational motion of the flames at the injector outlets, associated to asymmetric velocity field perturbations in the injector nozzles [33]. The capacity of flames to maintain the combustion process under intense transverse velocities induced by an acoustic mode was investigated by Lespinasse et al. [31], where it was shown that premixed "V" flames placed at a pressure nodal line are more sensitive to blow off than the same flames placed at a pressure antinodal line. For these flames, stabilized on a cylindrical rod having a diameter $d = 3$ mm placed in a premixed stream at a bulk velocity $U_b = 2$ m.s^{-1}, extinction was obtained, for example, at a pressure amplitude of 100 Pa at two resonance frequencies $f_0 = 506$ Hz and $f_0 = 1012$ Hz. The transverse velocity at the pressure node could be estimated to be about 0.2 m.s^{-1}, corresponding to 10% of the bulk velocity. The response of a linear array of swirling spray flames centered on a pressure antinode of a 2T1L resonant mode was examined in the new facility TACC-Spray [34], where the flames are stabilized aerodynamically and without the help of side walls.

Further references dealing with combustion instabilities and coupling with transverse acoustic modes are reviewed in [3]. It appears that there are no detailed investigations of the DBO process for swirling spray flames subjected to a transverse acoustic field. The objective of the present work is to bring new insight into this process by combining well controlled experiments with a theoretical framework initially proposed in [13] but modified in the present article.

This article begins with a brief description of the experimental configuration. The theoretical framework is introduced next and serves to guide the experimental investigation. Experiments confirm that flame blow out is observed when the pressure amplitude reaches high levels and when the flame is located near the transverse velocity antinodal line. Characteristic features of the dynamical blow out process are then examined in more detail for three mass flow rates of air.

2. Experimental setup and diagnostics

The TACC-Spray setup, shown in Fig. 3, comprises a rectangular chamber. The top of the chamber is surmounted by a convergent part which prevents the entrainment of surrounding air. Its exhaust is open to the atmosphere. An array of five injection units is mounted at the chamber backplane with a spacing that is equal to that used in the MICCA-Spray experiment. They are equipped with tangential swirlers of type 716, identical to those of MICCA-Spray (see [27] for further details about the swirler). The three central units inject air and a droplet spray of liquid n-heptane while the two lateral injectors only supply air, thus partially reproducing the aerodynamics in the side regions and acting as stabilizers of the lateral flames. This original arrangement where the lateral flames are well anchored far from the side walls, places the central flame in an environment reflecting that of MICCA-Spray at any location of the acoustic field. Two compression drivers Beyma CP850ND (marked as CD in Fig. 3) are fixed on the side walls, facing each other such that their common acoustic axis which passes through their centers is at 90 mm from the chamber backplane. They are characterized by a wide frequency range (0.5–20 kHz). The excitation signals are delivered by a Hameg HM8150 signal generator, an IMG Stageline frequency filter and a Peavey PV900 amplifier. Here, the 0-peak acoustic pressure amplitude P' is measured with B&K type

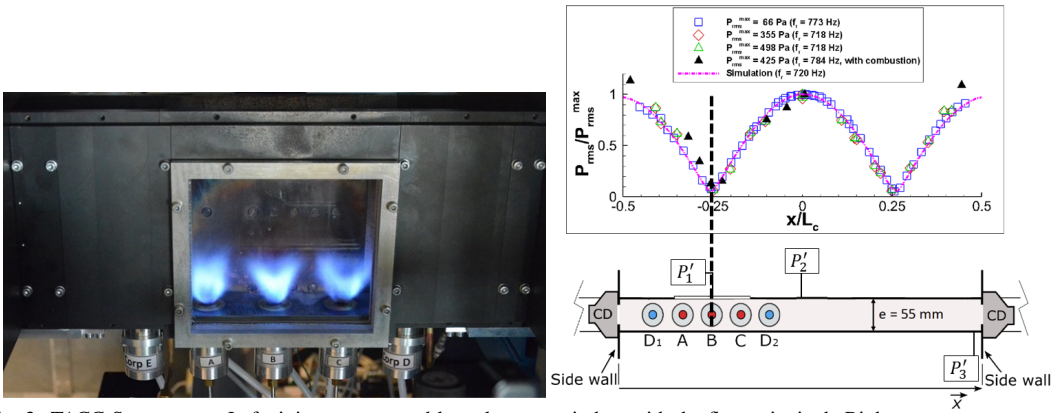

Fig. 3: TACC-Spray setup. Left: injector array and lateral quartz window with the flames ignited. Right: transverse acoustic field inside the cavity (top) and a schematic of the top view of TACC-Spray (bottom). The central flame (injector B) is at a velocity antinode (VAN). P_1', P_2' and P_3' are simultaneously obtained at VAN, central pressure antinode (PAN) and lateral PAN respectively.

4182 microphones plugged at several positions on the chamber front walls at 8 mm from the chamber backplane, as shown in Fig. 3. The vertical side walls holding the driver units are placed on rails and the front walls are made of plates of height $h_c = 200$ mm and different lengths, which allows to vary the chamber length L_c and ensure acoustic resonance at a selected frequency f for a frequency in the range 680-780 Hz, corresponding to the DBO frequency range in MICCA-Spray. A transverse mode is generated in the rectangular chamber, with peak amplitude levels that may reach 1700 Pa. This is used to locate the pressure, velocity or intensity antinode so that it coincides with the central injector. Global flame emission is observed with a photomultiplier Hamamatsu H10721-210 equipped with a UV-visible lens and an interference filter centered on OH* emission in the UV range ($\lambda = 305$ nm, FWHM = 24 nm). High-speed imaging of the OH* radical is performed at a rate of 10000 fps with a Phantom V2012 camera equipped with a Lambert HiCATT 25 intensifier, a UV-105 mm lens and a UG11 filter.

3. Theoretical framework

The general ideas that were followed in [13] to derive a theoretical model for the DBO phenomenon are now used to guide the blow out experiments in TACC-Spray. Blow out takes place when the central injector is located at a pressure node of the resonant acoustic field, where the transverse velocity v_x' reaches maximum values. The data from MICCA-Spray indicate that DBO requires high amplitude oscillations. It is also found that the transverse velocity induced by the acoustic field displaces the flames in the transverse direction. This modifies the heat release rate in the flames located near the pressure nodal line, where the transverse velocity reaches its maximum. In the initial model, the parameters influencing the blow out were as follows: injector exit diameter d, bulk velocity at the injector exit U_b, conversion time τ_c, transverse velocity fluctuation amplitude v_x', angular frequency $\omega = 2\pi f$, and the swirl number S. Parameter $\tau_c = \tau_m + \tau_v + \tau_{ch}$ includes a mixing time τ_m, a vaporization time τ_v and a chemical time τ_{ch}. Mixing is essentially governed by turbulence, vaporization depends on the droplet diameters and clustering in the spray, while the chemical conversion is a function of the local equivalence ratio ϕ. Dimensional analysis indicates that there are four dimensionless groups that may be written as v_x'/U_b, the relative velocity perturbation amplitude, $v_x'/(\omega d)$, the ratio of the transverse displacement to the injector outlet diameter, $(\tau_c U_b)/d$, the ratio of the chemical conversion time to a mechanical time d/U_b and S, the swirl number measuring the rate of rotation with respect to the axial flow velocity. The flame extinction is then formally governed by a criterion that may be cast in the form:

$$\psi_1\left(\frac{v_x'}{U_b}, \frac{v_x'}{\omega d}, \frac{\tau_c U_b}{d}, S\right) > 0 \qquad (1)$$

It was initially considered that the relative transverse displacement amplitude $v_x'/(\omega d)$ was governing the flame extinction process. When this ratio is sufficiently large, the central recirculation zone which anchors the flame is significantly perturbed, destabilizing the flame and inducing blow out. However, $v_x'/\omega d$ is dependent on v_x'/U_b and the inverse of the Strouhal number St defined by $\mathrm{St} = \omega d/U_b$. So, it may be interesting to replace the second dimensionless group by the Strouhal number. The influence of frequency on the process is then reflected by this important dimensionless number. The extinction condition may then be rewritten in the form:

$$\frac{v_x'}{U_b} > \psi_2\left(\mathrm{St}, \frac{\tau_c U_b}{d}, S\right) \qquad (2)$$

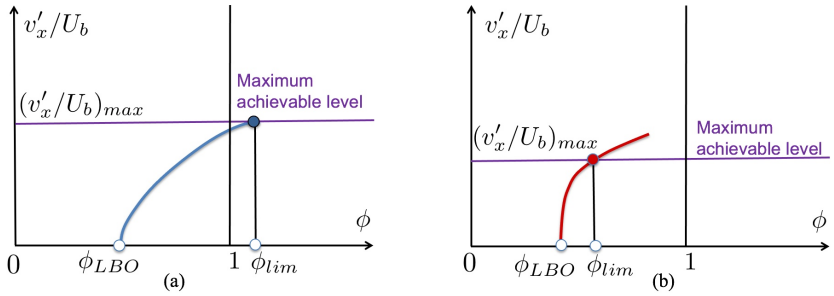

Fig. 4: Dynamical flame blow out conditions may be determined by changing the equivalence ratio to vary the stability margin. When this ratio reaches the lean blow out limit, the flame is extinguished. The range of equivalence ratios between ϕ_{LBO} and a limit value ϕ_{lim} may be explored and the level of transverse oscillation that leads to extinction may be determined. Beyond ϕ_{lim}, the level of transverse velocity fluctuation exceeds the maximum achievable value and this range cannot be explored. These diagrams only consider lean operating conditions. Left: Low bulk velocity case. The flame is not very well anchored and extinction may be observed over an extended range of equivalence ratios limited by the maximum achievable level of transverse velocity fluctuation. Right: High bulk velocity case. Flame anchoring is improved and the maximum achievable level of relative transverse velocity oscillation is reduced. The range of equivalence ratios in which DBO may be observed is diminished.

It is known that the parameter $(\tau_c U_b)/d$ that will be designated from here on by b, typically determines the stability of a combustion system. When this parameter is smaller than a critical value corresponding to static blow out, say b_* of the order of one, the conversion time is shorter than the mechanical time and the flame is stabilized. When b exceeds b_*, the flame is extinguished. This is equivalent to say that the Damköhler number should exceed a critical value for flame stabilization (*i.e.*, Da $>$ Da$_c$). The difference $b_* - b$ then measures the stability margin and may be used in place of the dimensionless group b. One may then separate the right hand side in expression (2) in two parts, the first reflecting the state of rotation and flow response $\psi_3(S, \mathrm{St})$ while the second represents the stability margin in the form $(b_* - b)^n$. The dynamical blow out criterion then takes the form:

$$\frac{v'_x}{U_b} > \psi_3(S, \mathrm{St})(b_* - b)^n \qquad (3)$$

This criterion slightly differs from that proposed in [13] in that it puts the accent on the transverse velocity disturbance and on the stability margin of the flame. The function ψ_3 portrays the swirling flow characterized by the swirl number S and its response to external modulations through a Strouhal number. For a fixed injector and a broadband receptivity to incident disturbances, one may consider that ψ_3 is a constant so that the criterion is essentially controlled by the stability margin $(b_* - b)^n$, where n may be obtained from experiments. If the flame is close to blow off, it may be easily perturbed by the external acoustic field. If the stability margin is greater, then the combustion process will be less easily perturbed. In the previous expression, $b = U_b \tau_c / d$ defines the stability of the flame and one may note that v'_x/U_b has to be sufficiently large if the acoustic field is to play a role and induce flame blow off. This analysis may be tested by changing the value of b to vary the stability margin of the flame. For a fixed injector geometry, this may be achieved by changing the bulk velocity U_b or by changing the conversion time τ_c. When τ_c is increased, the stability margin is reduced. It is most convenient to augment the chemical time by operating under leaner conditions, *i.e.*, by reducing the equivalence ratio and operating near the lean blow out limit. This is illustrated in Fig. 4.

Diagrams in Fig. 4 may be used to guide the exploration of the DBO phenomenon. The central idea is to explore flames that have a narrow margin with respect to the lean blow out limit. The acoustic level is fixed and the equivalence ratio is progressively decreased until flame blow out. This scheme is repeated for higher acoustic levels until the maximum achievable level is reached. The corresponding equivalence ratio ϕ_{lim} is that which requires the highest achievable level of pressure oscillation, *i.e.*, the highest level of transverse velocity fluctuation. Beyond that point, the system cannot provide a level of oscillation that will lead to blow out.

4. Flame blow out induced by high amplitude oscillations

It is now interesting to examine results of blow out experiments carried out for three different bulk velocities, calculated by dividing the air mass flow rates by the ambient air density at 20°C and by the injector exit surface area (diameter $d = 8$ mm). The corresponding blow out boundaries are plotted in Fig. 5. The transverse velocity amplitude, v'_x corresponds to the theoretical value $P'_2/\rho_0 c_0$, with P'_2 obtained from experiments. This correspondence is well verified by evaluating the flame displacement by means of the high-speed OH* images. When the bulk velocity is low ($U_b = 17.8$ m/s) corresponding to the blue line, the maximum level of fluctuation can reach a value of 32 %. The flame is also not very well anchored because atomization produces bigger droplets, increasing the vaporization time and reducing the Damköhler

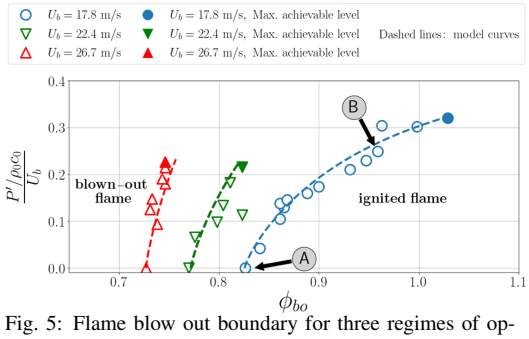

Fig. 5: Flame blow out boundary for three regimes of operation. Swirler type: 716, liquid n-heptane fuel. The blue symbols correspond to $U_b = 17.8$ m/s, $f = 745 - 760$ Hz, the green symbols to $U_b = 22.4$ m/s, $f = 755$ Hz and the red symbols correspond to $U_b = 26.7$ m/s, $f = 750 - 762$ Hz. Filled symbols indicate the maximum achievable level of $P_2'/(\rho_0 c_0 U_b)$. A and B indicate operating conditions that are analyzed in the text. Theoretical curves shown as dashed lines are obtained with $n = 0.8$.

number. In this case, transverse acoustic oscillations induce blow out at equivalence ratios as high as 1.03. This situation corresponds to that shown schematically in Fig. 4 (left). When the bulk velocity is increased, atomization is improved, vaporization time is reduced and flame anchoring is enhanced. The maximum achievable level of velocity fluctuation is reduced to about 20% for $U_b = 26.7$ m/s, so DBO is observable in a more limited range of equivalence ratios, as shown schematically in Fig. 4 (right). To assess the theoretical model, b_* (without acoustics), b at the maximum achievable level and ψ_3 of eq. (3) are obtained by making use of values of τ_c deduced from flame stabilization experimental data [35], expressed as a function of ϕ. Those data correspond to experiments carried out under premixed conditions in a situation where the flame was anchored by hot gas recirculation behind a buff-body. In that case, the characteristic time τ_c only depended on the equivalence ratio ϕ. In the present case, the flame is stabilized by hot products that are recirculated by the rotating flow, and the characteristic time τ_c also accounts for a delay associated with vaporization. It is then necessary to use the general trends with respect to ϕ defined in [35] but shift the data, thus including a dependency on this vaporization time. This is guided by the fact that flame blow off in the absence of acoustic modulation is a function of the bulk velocity. The curves derived from the model are in good agreement with the experimental data for $n = 0.8$ for the three operating points.

For $U_b = 17.8$ m/s, the DBO limit curve presents a changing slope, showing a limited sensitivity to acoustics for low acoustic amplitudes, which is accentuated when U_b is increased. Indeed, blow out at $U_b = 26.7$ m/s occurs almost at the same equivalence ratio without acoustics and for a relative velocity perturbation of 20%, which is not observed for the lower value of the bulk velocity. The blow out process is detected when the OH* light emission captured by the photomultiplier drops down to zero. This is illustrated in Fig. 6 which shows light intensity records for the central flame. The system operates at $U_b = 17.8$ m/s. The signal recorded in the absence of acoustics characterizes a typical blow out event at $\phi = 0.83$. The second signal recorded at an equivalence ratio of $\phi = 0.96$ exemplifies a dynamic blow out induced by a relative pressure fluctuation $P'/\rho_0 c_0 U_b = 24\%$, where the air density ρ_0 and sound velocity c_0 are determined at the microphone location. These two signals correspond to points A and B in Fig. 5. In the absence of acoustics, blow out of the whole system is induced by the total extinction of any of the three flames, but the partial extinction of any of the three flames does not necessarily provoke the whole system extinction. There, the central flame undergoes many partial extinctions of short duration when the system operates in the vicinity of its stability limit. These events are identified by pronounced reductions of the OH*-intensity, which drops down to zero, as shown at times $t_{BO} - 2.85$ s and $t_{BO} - 1.9$ s. Each partial extinction lasts for less than 70 ms, after which the flame is reignited. Finally, a complete blow-out occurs when the partial extinction exceeds 50 to 70 ms. In the presence of an adequate acoustic level, it is only the central flame at VAN which first blows out, leading to the extinction of the whole system a short time later. Two behaviors are observed in this case, highlighted by the change in the slope of the DBO limit curve. In the region pertaining to the smaller acoustic fluctuation levels, characterized by a nearly vertical boundary between ignited flames and blown-out flames (see Fig. 5), the extinction process is quite similar to that observed in the absence of acoustics. For these lower acoustic amplitudes, DBO is mainly induced by standard mechanisms of lean blow out. As the equivalence ratio is increased, stabilization is improved, and a greater acoustic amplitude is required to blow out the flame. In the region corresponding to the weaker slope of the blow out boundary, partial extinctions appear when the point of operation approaches the DBO limit curve. These extinction events are less common as the acoustic amplitude increases, as found by a statistical analysis of the OH* signals during time intervals of 8000 - 10000 acoustic cycles preceding blow out. This is illustrated in Fig. 6 for $\phi = 0.96$, in which a single partial extinction of one part of the flame is detected just before blow out occurs, the PM-signal recorded for 4 seconds showing no other partial extinction event, while for $\phi = 0.83$, five partial extinctions are identified during the same time span. When the equivalence ratio is augmented, flame anchoring is enhanced, and DBO requires higher acoustic amplitudes inducing stronger transverse velocities. The ability of the flame to reignite after undergoing such a strong partial extinction is then impeded, as seen in Fig. 6.

The DBO process for the low bulk velocity case is examined by making use of time-resolved high-

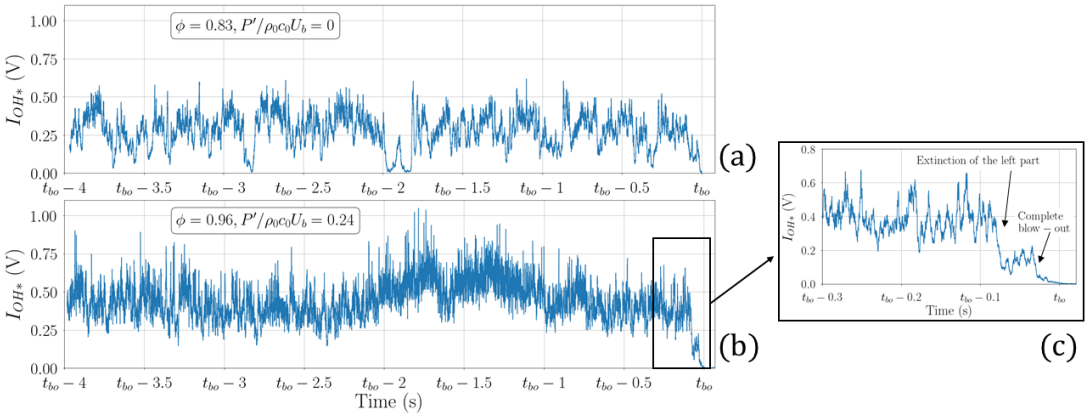

Fig. 6: OH* signals of the whole central flame during 4 seconds before DBO for $U_b = 17.8$ m/s: (a) Light emission during a typical blow out at $\phi = 0.83$, in the absence of acoustic modulation; (b) Dynamical blow out obtained at $\phi = 0.96$ with an acoustic modulation level $P'_2/(\rho_0 c_0 U_b) = 0.24$ at a frequency $f = 760$ Hz; (c) A detailed view of the last signal during the final period.

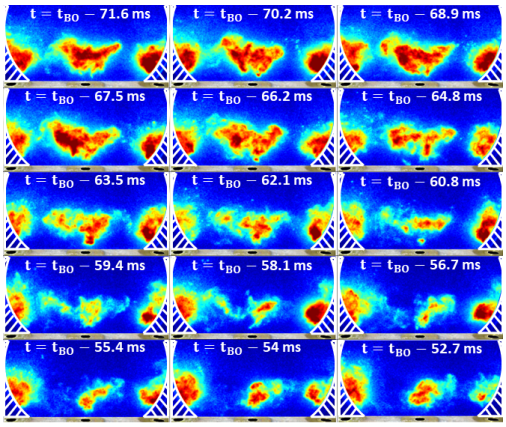

Fig. 7: Images of step 1 of the flame blow out process extracted from a high speed film recorded at 10000 fps for $U_b = 17.8$ m/s, $\phi = 0.96$, $f = 760$ Hz. Time t is counted down and indicates the time before complete blow out of the central flame. Successive images are presented from left to right and top to bottom. Flames cannot be observed in the white dashed regions.

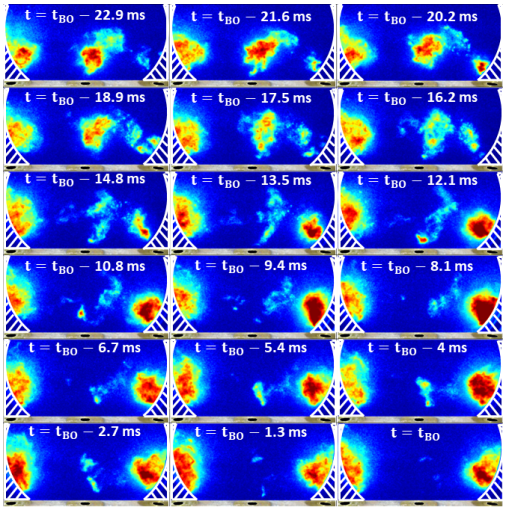

Fig. 8: Images of the step 3 of the flame blow out process extracted from a high speed film recorded at 10000 fps for $U_b = 17.8$ m/s, $\phi = 0.96$, $f = 760$ Hz. Time t is counted down and indicates the time before complete blow out of the central flame. Successive images are presented from left to right and top to bottom. Flames cannot be observed in the white dashed regions.

speed OH*-emission images. All image sequences captured with acoustics show the total extinction of the central flame located at the pressure node, retrieving the DBO phenomenon observed in MICCA-Spray (for $\phi = 1.06$). The DBO process driven by acoustic effects is achieved in three successive steps where the front-interaction between the central flame and one of the lateral flames plays an important role, favored by the transverse flame displacement induced by the acoustic velocity. This is illustrated in Figs. 7 and 8 for ϕ = 0.96 and $P'/\rho_0 c_0 U_b = 24\%$ (case (b) of Fig. 6) where flame interactions take place between the central and lateral right flames. *Step 1* (see Fig. 7) corresponds to the partial extinction of the central flame with a net reduction of light emission from its left part, reflecting a reduction in the global heat release rate. This affects the flame stabilization mechanism by facilitating the penetration of a greater amount of burnt gases diluting fresh reactants in the flame anchoring region. Simultaneously, the right part of the central flame becomes weaker, featuring a fragmentation in lumps at $t = t_{BO} - 60.8$ ms. During *step 2*, the weakened flame persists and remains ignited until $t = t_{BO} - 22.9$ ms by interacting

here with the left part of the lateral right flame, which is also seen to become less intense during this interval. *Step 3*: from $t = t_{BO} - 22.9$ ms (see Fig. 8), the central flame progressively extinguishes by its downstream part. At the same time, the OH*-intensity of the left part of the lateral right flame increases again such that it reaches a similar level to the one observed for $t < t_{BO} - 60$ ms, showing the ability of the lateral flame to fully reignite from a weakened state. This process is facilitated by the strong displacement of the central flame. The central flame stabilization point is occasionally reactivated, as shown by the presence of puffs of OH* at $t = t_{BO} - 12.1$ ms and $t = t_{BO} - 5.4$ ms, but the associated heat release rate is unable to allow reignition of the entire flame and the presence of the lateral flames is not sufficient to maintain the central flame. Therefore, the lower resistance to blow out of the central flame results from the stronger transverse velocity at the pressure node.

5. Conclusion

Experiments have been carried out in a system comprising an array of swirling injectors fed with liquid n-heptane and air placed in a rectangular configuration operating at atmospheric pressure. This configuration may be modulated by transverse acoustic modes generated by a set of driver units located on the lateral sides of the system. The pressure oscillation may reach peak values of the order of 1700 Pa peak (about 2% of the chamber pressure). Experiments reveal that these high acoustic levels induce a strong transverse motion in the neighborhood of the pressure nodal line which also corresponds to a maximum in transverse velocity fluctuations. Experiments indicate that the combustion process markedly changes when the position of the central injector coincides with a pressure antinode or when it corresponds to a nodal line. In this latter case, when the pressure oscillation amplitude exceeds a certain threshold, the flame senses maximum transverse velocity fluctuations that produce a dynamical extinction. A mechanism is proposed for this flame extinction process that defines a critical value for the transverse velocity amplitude with respect to the injection velocity. The blow out limit boundary highlights two extinction regimes, in which blow out is dominated either by standard mechanisms leading to lean blow out, or by transverse velocity oscillations. In the latter case, partial extinctions of the central flame lead to irreversible flame blow out, while lateral flames can be maintained even after complete blow out of the central flame. The data reported in this article provide new insights on the dynamical blow out that results from excessive levels of acoustic oscillation and may serve to guide modeling and simulation of interactions between acoustics and combustion.

Acknowledgements

This work was partially supported by project FASMIC (ANR16-CE22-0013) of the French National Research Agency (ANR), and by the European Union's Horizon 2020 research and innovation programme, "Annulight" with grant agreement no. 765998. The authors wish to thank RENADIAG for the technical support provided to this research.

References

[1] S. Candel, Combustion dynamics and control: progress and challenges., Proceedings of the Combustion Institute 29 (1) (2002) 1–28.

[2] Y. Huang, V. Yang, Dynamics and stability of lean-premixed swirl-stabilized combustion, Progress in Energy and Combustion Science 35 (4) (2009) 293–364.

[3] J. O'Connor, V. Acharya, T. Lieuwen, Transverse combustion instabilities: Acoustic, fluid mechanic, and flame processes, Progress in Energy and Combustion Science 49 (2015) 1–39.

[4] T. Poinsot, Prediction and control of combustion instabilities in real engines, Proceedings of the Combustion Institute 36 (1) (2017) 1–28.

[5] D. Fanaca, P. R. Alemela, C. Hirsch, T. Sattelmayer, Comparison of the Flow Field of a Swirl Stabilized Premixed Burner in a Annular and a Single Burner Combustion Chamber, Journal of Engineering for Gas Turbines and Power 132 (7) (2010) 071502.

[6] J. P. Moeck, M. Paul, C. O. Paschereit, Thermoacoustic Instabilities in an Annular Rijke Tube, in: ASME Conference Proceedings, Paper GT 2010-23577, Glasgow, UK, 2010.

[7] N. A. Worth, J. R. Dawson, Self-excited circumferential instabilities in a model annular gas turbine combustor: Global flame dynamics, Proceedings of the Combustion Institute 34 (2) (2013) 3127–3134.

[8] N. A. Worth, J. R. Dawson, Modal dynamics of self-excited azimuthal instabilities in an annular combustion chamber, Combustion and Flame 160 (11) (2013) 2476–2489.

[9] J.-F. Bourgouin, D. Durox, T. Schuller, J. Beaunier, S. Candel, Ignition dynamics of an annular combustor equipped with multiple swirling injectors, Combustion and Flame 160 (8) (2013) 1398–1413.

[10] J.-F. Bourgouin, D. Durox, J. Moeck, T. Schuller, S. Candel, Self-sustained instabilities in an annular combustor coupled by azimuthal acoustic modes, in: Proceedings of ASME Turbo Expo, Paper GT2013-95010, San Antonio, Texas, USA, 2013.

[11] N. A. Worth, J. R. Dawson, J. A. M. Sidey, E. Mastorakos, Azimuthally forced flames in an annular combustor, Proceedings of the Combustion Institute 36 (3) (2016) 3783–3790.

[12] K. Prieur, D. Durox, T. Schuller, S. Candel, A hysteresis phenomenon leading to spinning or standing azimuthal instabilities in an annular combustor, Combustion and Flame 175 (2017) 283–291.

[13] K. Prieur, D. Durox, T. Schuller, S. Candel, Strong Azimuthal Combustion Instabilities in a Spray Annular Chamber With Intermittent Partial Blow-Off, Journal of Engineering for Gas Turbines and Power 140 (3) (2018) 031503.

[14] S. Evesque, W. Polifke, C. Pankiewitz, Spinning and azimuthally standing acoustic modes in annular combustors, in: AIAA Conference Proceedings Paper 2003-3182, 2003.

[15] G. Ghirardo, M. Juniper, Azimuthal instabilities in annular combustors: standing and spinning modes, Proceedings of the Royal Society A: Mathematical, Physical and Engineering Science 469 (2013) 2013032.

[16] N. Noiray, B. Schuermans, On the dynamic nature of azimuthal thermoacoustic modes in annular gas turbine combustion chambers, Proceedings of the Royal Society A: Mathematical, Physical and Engineering Science 469 (2013) 20120535.
[17] M. Bauerheim, J.-F. Parmentier, P. Salas, F. Nicoud, T. Poinsot, An analytical model for azimuthal thermoacoustic modes in an annular chamber fed by an annular plenum, Combustion and Flame 161 (2014) 1374–1389.
[18] M. Bauerheim, P. Salas, F. Nicoud, T. Poinsot, Symmetry breaking of azimuthal thermo-acoustic modes in annular cavities: a theoretical study, Journal of Fluid Mechanics 760 (2014) 431–465.
[19] G. Ghirardo, M. Juniper, J. P. Moeck, Weakly nonlinear analysis of thermoacoustic instabilities in annular combustors, Journal of Fluid Mechanics 805 (2015) 52–87.
[20] M. Bothien, N. Noiray, B. Schuermans, Analysis of azimuthal thermo-acoustic modes in annular gas turbine combustion chambers, Journal of Engineering for Gas Turbines and Power 137 (2015) 061505.
[21] D. Laera, T. Schuller, K. Prieur, D. Durox, S. M. Camporeale, S. Candel, Flame Describing Function analysis of spinning and standing modes in an annular combustor and comparison with experiments, Combustion and Flame 184 (2017) 136–152.
[22] J. P. Moeck, D. Durox, T. Schuller, S. Candel, Nonlinear thermoacoustic mode synchronization in annular combustors, Proceedings of the Combustion Institute 37 (4) (2019) 5343–5350.
[23] P. Wolf, R. Balakrishnan, G. Staffelbach, L. M. Gicquel, T. Poinsot, Using LES to Study Reacting Flows and Instabilities in Annular Combustion Chambers, Flow, Turbulence and Combustion 88 (1-2) (2012) 191–206.
[24] P. Wolf, G. Staffelbach, L. Gicquel, J.-D. Müller, T. Poinsot, Acoustic and large eddy simulation studies of azimuthal modes in annular combustion chambers, Combustion and Flame 159 (2012) 3398–3413.
[25] J.-F. Bourgouin, D. Durox, J. P. Moeck, T. Schuller, S. Candel, A new pattern of instability observed in an annular combustor: The slanted mode, Proceedings of the Combustion Institute 35 (3) (2015) 3237–3244.
[26] J.-F. Bourgouin, D. Durox, J. P. Moeck, T. Schuller, S. Candel, Characterization and modelling of a spinning thermoacoustic instability in an annular combustor equipped with multiple matrix injectors, Journal of Engineering for Gas Turbines and Power 137 (2015) 021503.
[27] G. Vignat, D. Durox, A. Renaud, S. Candel, High amplitude combustion instabilities in an annular combustor inducing pressure field deformation and flame blow-off, Journal of Engineering for Gas Turbines and Power 142 (2020) 011016.
[28] J. O'Connor, T. Lieuwen, Disturbance field characteristics of a transversely excited burner, Combustion Science and Technology 183 (5) (2011) 427–443.
[29] J. O'Connor, T. Lieuwen, Further characterization of the disturbance field in a transversely excited swirl-stabilized flame, Journal of Engineering for Gas Turbines and Power 134 (2012) 011501.
[30] W. Y. Kwong, A. M. Steinberg, Effect of internozzle spacing on lean blow-off of a linear multinozzle combustor, Journal of Propulsion and Power 36 (4) (2020) 540–550.
[31] F. Lespinasse, F. Baillot, T. Boushaki, Responses of v-flames placed in an hf transverse acoustic field from a velocity to pressure antinode, Comptes Rendus Mécanique 341 (1) (2013) 110–120.
[32] F. Baillot, F. Lespinasse, Response of a laminar premixed v-flame to a high-frequency transverse acoustic field, Combustion and Flame 161 (5) (2014) 1247–1267.
[33] M. Hauser, M. Lorenz, T. Sattelmayer, Influence of transversal acoustic excitation of the burner approach flow on the flame structure, Journal of Engineering for Gas Turbine and Power 133 (2011) 041501.
[34] F. Baillot, C. Patat, M. Caceres, J. Blaisot, E. Domingues, Saturation phenomenon of swirling spray flames at pressure antinodes of a transverse acoustic field, Proceedings of the Combustion Institute 38 (5) (2021) 5987–5995.
[35] E. E. Zukoski, Aerothermodynamics of Aircraft Engine Components, Chapter 2: Afterburners, AIAA, 1985.